DALTON
FULL PAPER

Dinuclear zinc(II) complex of a new acyclic phenol-based dinucleating ligand with four methoxyethyl chelating arms: first dizinc model with aminopeptidase function

Hiroshi Sakiyama,*[a] Rieko Mochizuki,[a] Akihiko Sugawara,[a] Masatomi Sakamoto,[a] Yuzo Nishida[a] and Mikio Yamasaki[b]

[a] Department of Material and Biological Chemistry, Faculty of Science, Yamagata University, Kojirakawa, Yamagata 990-8560, Japan. E-mail: saki@sci.kj.yamagata-u.ac.jp
[b] X-Ray Research Laboratory, Rigaku Corporation, 3-9-12 Matsubara, Akishima, Tokyo 196-8666, Japan

A new end-off type acyclic ligand with four methoxyethyl chelating arms, 2,6-bis[bis(2-methoxyethyl)aminomethyl]-4-methylphenol (Hbomp), formed a dinuclear zinc(II) complex [Zn$_2$(bomp)(MeCO$_2$)$_2$]BPh$_4$ **1**. X-Ray analysis revealed that the complex **1**·CHCl$_3$ contains two zinc ions bridged by the phenolic oxygen and two acetate groups, forming a μ-phenoxo-bis(μ-acetato)dizinc(II) core. The aminopeptidase function of complex **1** was estimated using N-p-nitrophenyl-L-leucine as substrate. The release of p-nitroaniline as the result of the substrate hydrolysis is first order in both complex and substrate concentrations with $k = 2.3(1) \times 10^{-3}$ dm^3 mol^{-1} s^{-1}.

Introduction

Dinuclear zinc(II) cores are often seen in biological systems, such as phosphatases[1,2] and aminopeptidases.[3–5] In addition, some synthetic dinuclear zinc(II) complexes are found to have functions in RNA hydrolysis[6] and dephosphorylation.[7] In order not only to mimic the core structure found in biological systems, but also to achieve the biological function, the development of multinucleating ligands is of importance. 2,6-Bis-[bis(2-pyridylmethyl)aminomethyl]-4-methylphenol (Hbpmp) is one of the most well known dinucleating ligands, first reported by Suzuki et al.[8] This ligand is acyclic, and consists of a phenolate head unit, two aminomethyl shoulders and four pyridylmethyl arms, forming two N$_3$O co-ordination sites. It and its derivatives are reported to stabilize various homo- and hetero-dinuclear cores.[9] N,N'-2-Hydroxy-5-methyl-1,3-xylylenebis-[N-(methoxycarbonyl)glycine] [H$_5$(5-Me-hxta)], reported by Que and co-workers,[10] is also a well known acyclic dinucleating ligand. This has four methoxycarbonyl chelating arms, possessing two NO$_3$ co-ordination sites. It functions as a pentavalent anionic ligand, and most of its dinuclear metal complexes are soluble in water. Both bpmp$^-$ and 5-Me-hxta^{5-} are end-off type acyclic dinucleating ligands suitable for incorporating various dinuclear cores. Furthermore, complexes with these ligands are stable in aqueous media since these ligands are stable to water, whereas Schiff base type ligands are hydrolysed in the presence of water.

In this study a new acyclic dinucleating ligand 2,6-bis[bis(2-methoxyethyl)aminomethyl]-4-methylphenol (Hbomp) is synthesized with the intention of developing functional model complexes containing a dinuclear core. It has one minus charge as bpmp$^-$ and two NO$_3$ donor sets as does 5-Me-hxta^{5-}. The ligand is expected to form dinuclear metal complexes which are stable in aqueous media during some catalytic processes. It will be interesting to develop new functional models with this new ligand system since properties of dinuclear metal complexes are strongly influenced by the nature of the ligand.

Phosphatases are enzymes that hydrolyse phosphomonoesters. At present structures of alkaline phosphatase[1] (ALP, EC 3.1.3.1) and fructose-1,6-bisphosphatase[2] (FBPase, EC 3.1.3.11) containing dinuclear zinc(II) cores have been deter-

bomp$^-$ H$_5$ (5-Me-hxta)
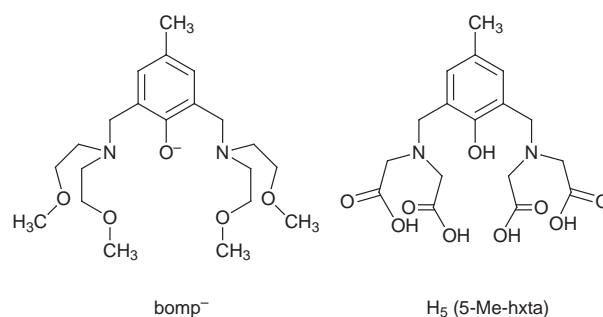
mined: ALP hydrolyses phosphate esters, optimally at high pH; FBPase, a regulatory enzyme in gluconeogenesis, catalyses the hydrolysis of fructose 1,6-bisphosphate to fructose 6-phosphate. Aminopeptidases are enzymes that remove the N-terminal amino acid from a protein or peptide. All those that have been structurally determined contain dinuclear cores at their active sites, while carboxypeptidases, which remove the C-terminal amino acid, do not have any dinuclear cores. At present three types of aminopeptidases are structurally characterized: leucine aminopeptidase[3] (LAP, EC 3.4.11.1), methionine aminopeptidase[4] (MAP, EC 3.4.11.18) and aminopeptidase from Aeromonas proteolytica[5] (AAP, EC 3.4.11.10). The LAP and AAP contain a μ-hydroxo-bis(μ-carboxylato)dizinc(II) core and a μ-aqua-μ-carboxylato-dizinc(II) core at their active sites, respectively, whereas MAP contains a bis(μ-carboxylato)dicobalt(II) core. The mechanism of aminopeptidase function has been well studied for LAP[11] and AAP,[12] and the "two-metal ion mechanism" has been proposed for both enzymes although the substrate incorporation modes differ from each other.

One of our purposes is to reveal why a dinuclear metal core is necessary for aminopeptidases but not for carboxypeptidases. In this study we intended to develop a synthetic dizinc model possessing an aminopeptidase function as the first step for the functional modelling. A new dinuclear zinc(II) complex [Zn$_2$-(bomp)(MeCO$_2$)$_2$]BPh$_4$ **1** was synthesized using our new ligand, and the aminopeptidase function examined. Complex **1** contains a μ-phenoxo-bis(μ-acetato)dizinc(II) core, similar to those

found in aminopeptidases, and this is the first dizinc model with an aminopeptidase function as far as we know.

Experimental

Measurements

Elemental analyses were obtained at the Elemental Analysis Service Centre of Kyushu University. Infrared (IR) spectra were recorded on a Hitachi 270-50 spectrometer, ^{1}H NMR spectra (400 MHz) on a JEOL JNM-α400 spectrometer in CDCl$_3$ using SiMe$_4$ as the internal standard, fast atom bombardment (FAB) mass spectra on a Fisons ZabSpec Q mass spectrometer in dimethylformamide (dmf) with a glycerol matrix and electronic spectra on a Shimadzu UV-2200 spectrometer. All chemicals were commercial products used as supplied.

Preparations

Na(bomp). To an aqueous solution (50 ml) containing *p*-cresol (5.41 g, 50 mmol), NaOH (2.00 g, 50 mmol) and bis(2-methoxyethyl)amine (13.32 g, 100 mmol) were added formaldehyde solution (37%, 7.8 ml, 100 mmol) and ethanol (20 ml) and the resulting solution was refluxed for 1 h. After evaporation to dryness the resulting oily products were extracted with diethyl ether. Ether was removed by evaporation to give Na(bomp) as a colourless oil. Yield 4.84 g (23%). Selected IR data ($\tilde{v}$/cm^{-1}) using NaCl plates: 2980–2820, 1680, 1610, 1500, 1480–1450, 1360, 1250, 1190, 1110, 1010 and 820. ^{1}H NMR in CDCl$_3$: δ 2.23 (s, 3 H), 2.83 (t, 8 H), 3.33 (s, 12 H), 3.54 (t, 8 H), 3.81 (s, 4 H) and 6.91 (s, 2 H). FAB mass spectrum: *m/z* 399, [H$_2$(bomp)]$^+$; 421, [NaH(bomp)]$^+$; and 443, [Na$_2$(bomp)]$^+$.

[Zn$_2$(bomp)(MeCO$_2$)$_2$]BPh$_4$ 1. To a methanolic solution (15 ml) of Na(bomp) (0.21 g, 0.50 mmol) was added zinc(II) acetate dihydrate (0.22 g, 1.0 mmol), and the resulting solution was refluxed for 1 h to give a yellow solution. The addition of sodium tetraphenylborate (0.17 g, 0.50 mmol) resulted in the precipitation of white microcrystals. Yield 0.32 g (65%) (Found: C, 60.70; H, 6.55; N, 2.90; Zn, 12.4. Calc. for C$_{49}$H$_{63}$BN$_2$O$_9$Zn$_2$: C, 60.95; H, 6.60; N, 2.90; Zn, 13.5%). Selected IR data ($\tilde{v}$/cm^{-1}) using KBr disks: 3050–2900, 1950–1750, 1610, 1480–1430, 1200, 1100, 740 and 710. ^{1}H NMR in CDCl$_3$: δ 2.01 (s, 6 H), 2.22 (s, 3 H), 2.52–2.80 (br, 8 H), 3.22 (s, 12 H), 3.27 (m, 8 H), 3.59 (br, 4 H), 6.81 (s, 2 H), 6.91 (t, 4 H), 7.06 (t, 8 H) and 7.43 (m, 8 H).

Single crystal X-ray analysis of complex 1·CHCl$_3$

Crystal data. C$_{50}$H$_{64}$BCl$_3$N$_2$O$_9$Zn$_2$, M = 1084.99, triclinic, space group $P\bar{1}$ (no. 2), a = 14.626(1), b = 16.343(2), c = 13.398(1) Å, α = 99.200(2), β = 114.834(1), γ = 69.368(4)°, U = 2719.7(4) Å^3, D_c = 1.325 g cm^{-3}, Z = 2, $F(000)$ = 1132.00, μ(Mo-Kα) = 10.81 cm^{-1}.

Data collection and reduction. Single crystals of complex 1·CHCl$_3$ were obtained by the slow diffusion of propan-2-ol into a chloroform solution of **1**. A clear platelet crystal having approximate dimensions 0.56 × 0.30 × 0.16 mm was mounted on a glass fiber. All measurements were made on a RASA-7 Quantum CCD area detector with graphite-monochromated Mo-Kα radiation (λ = 0.71069 Å). The data were collected at 24 ± 1 °C to a maximum 2θ value of 55.0°. Of the 24447 reflections collected, 11605 were unique (R_{int} = 0.023). Azimuthal scans of several reflections indicated no need for an absorption correction. The data were corrected for Lorentz-polarization effects.

The structure was solved by direct methods[13] and expanded using Fourier techniques.[14] The chloroform molecule was disordered (6:4), and refined isotropically. Hydrogen atoms were
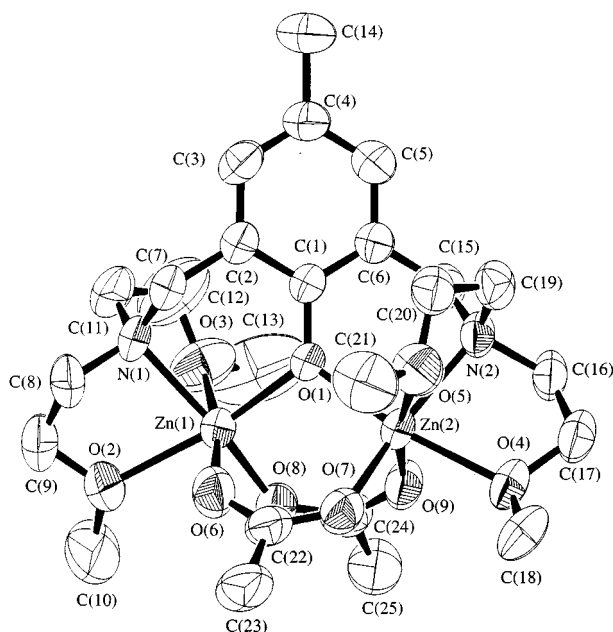
Fig. 1 An ORTEP[17] view of the complex cation [Zn$_2$(bomp)(MeCO$_2$)$_2$]$^+$ with the atom numbering scheme.

included but not refined. Refinement was carried out by the full-matrix least-squares method, where the function minimized was $\Sigma w(|F_o| - |F_c|)^2$. The final cycle of the refinement was based on 6909 observed reflections [$I > 3.00\sigma(I)$], and the final values of R and R' were 0.056 and 0.086, respectively. Neutral atom scattering factors were taken from Cromer and Waber.[15] All calculations were performed using the TEXSAN.[16]

CCDC reference number 186/1332.

See http://www.rsc.org/suppdata/dt/1999/997/ for crystallographic files in .cif format.

Aminopeptidase activity

The aminopeptidase activity of the complex was estimated using *N-p*-nitrophenyl-L-leucine [(CH$_3$)$_2$CHCH$_2$CH(NH$_2$)CO-NHC$_6$H$_4$NO$_2$] as substrate. Kinetic measurements were made as follows. *N-p*-Nitrophenyl-L-leucine was dissolved in 1.5 ml of Tricine buffer solution (pH 8), and to this was added 1.0 ml of dmf solution containing complex **1** at room temperature. Hydrolysis of *N-p*-nitrophenyl-L-leucine into L-leucine and *p*-nitroaniline was monitored by detecting the formation of the latter using a spectrometer at 405 nm. This measurement was made at various complex concentrations in the range from 0 to 2.0 × 10^{-4} mol dm^{-3} and at various substrate concentrations in the range from 0 to 4.0 × 10^{-4} mol dm^{-3}.

Results and discussion

Crystal structure of complex 1·CHCl$_3$

The crystal structure consists of [Zn$_2$(bomp)(MeCO$_2$)$_2$]$^+$ complex cations, tetraphenylborate anions and disordered chloroform molecules in a 1:1:1 molar ratio (Fig. 1). Selected distances and angles with their estimated standard deviations are listed in Table 1. The complex cation consists of one dinucleating ligand bomp$^-$, two zinc(II) ions and two acetate groups. The two zinc ions are bridged by the one phenolic oxygen of the dinucleating ligand and the two acetate ions, forming a μ-phenoxo-bis(μ-acetato)dizinc(II) core structure. The Zn(1)···Zn(2) separation is 3.2644(7) Å.

Atom Zn(1) has a six-co-ordinate distorted octahedral geometry with O(1), O(2), O(3) and N(1) of bomp$^-$ and O(6) and O(8) of the two acetate groups. The co-ordination geometry around Zn(2) is also distorted octahedral with O(1), O(4),

Table 1 Selected distances (Å) and angles (°) for complex **1**·CHCl₃

Zn(1)–O(1)	1.995(4)	Zn(2)–O(1)	2.003(3)
Zn(1)–O(2)	2.214(5)	Zn(2)–O(4)	2.197(3)
Zn(1)–O(3)	2.362(4)	Zn(2)–O(5)	2.440(3)
Zn(1)–O(6)	2.045(4)	Zn(2)–O(7)	1.979(4)
Zn(1)–O(8)	1.985(3)	Zn(2)–O(9)	2.048(2)
Zn(1)–N(1)	2.148(4)	Zn(2)–N(2)	2.146(4)
Zn(1)···Zn(2)	3.2644(7)		
O(1)–Zn(1)–O(2)	167.1(1)	O(1)–Zn(2)–O(4)	169.2(2)
O(1)–Zn(1)–O(3)	96.1(2)	O(1)–Zn(2)–O(5)	96.4(1)
O(1)–Zn(1)–O(6)	93.3(2)	O(1)–Zn(2)–O(7)	100.7(1)
O(1)–Zn(1)–O(8)	100.9(1)	O(1)–Zn(2)–O(9)	93.6(1)
O(1)–Zn(1)–N(1)	91.4(2)	O(1)–Zn(2)–N(2)	90.5(1)
O(2)–Zn(1)–O(3)	87.0(2)	O(4)–Zn(2)–O(5)	82.2(1)
O(2)–Zn(1)–O(6)	83.3(2)	O(4)–Zn(2)–O(7)	89.8(1)
O(2)–Zn(1)–O(8)	91.9(2)	O(4)–Zn(2)–O(9)	87.2(1)
O(2)–Zn(1)–N(1)	77.1(2)	O(4)–Zn(2)–N(2)	78.7(1)
O(3)–Zn(1)–O(6)	170.3(2)	O(5)–Zn(2)–O(7)	84.1(1)
O(3)–Zn(1)–O(8)	83.1(1)	O(5)–Zn(2)–O(9)	169.0(1)
O(3)–Zn(1)–N(1)	76.1(1)	O(5)–Zn(2)–N(2)	74.3(1)
O(6)–Zn(1)–O(8)	97.3(1)	O(7)–Zn(2)–O(9)	98.6(1)
O(6)–Zn(1)–N(1)	101.5(1)	O(7)–Zn(2)–N(2)	156.7(1)
O(8)–Zn(1)–N(1)	156.8(1)	O(9)–Zn(2)–N(2)	101.0(1)
Zn(1)–O(1)–Zn(2)	109.4(1)		

O(5) and N(2) of bomp⁻ and O(7) and O(9) of the two acetate groups. The geometries around Zn(1) and Zn(2) are very similar to each other, and the complex cation has a pseudo-C_2 axis along C(14), C(4), C(1) and O(1). The least-squares plane of the aromatic ring of bomp⁻ and the plane defined by Zn(1), Zn(2) and O(1) are twisted with a dihedral angle of 41.9°. The bond distances between zinc atoms and axial ether oxygens [2.362(4)–2.440(3) Å] are longer than those between zinc atoms and equatorial ether oxygens [2.197(3)–2.214(5) Å].

General properties of complex 1

The IR spectrum of complex **1** shows the antisymmetric and symmetric $v(CO_2)$ vibrations of the acetate group at 1610 and 1445 cm⁻¹, respectively. The Δv value [$\Delta v = v_{asym}(CO_2) - v_{sym}(CO_2)$] smaller than 200 cm⁻¹ is typical of a bridging carboxylate group.[18] This indicates **1** has a μ-phenoxo-bis(μ-acetato)dizinc(II) core structure as revealed using X-ray crystallography. Complex **1** shows no appreciable absorption in the region above 340 nm in dmf solution, in accord with the d¹⁰ electronic configuration of the zinc(II) ion. In the FAB mass spectrum of **1** in dmf the most predominant ions appeared at *m*/*z* 643, 645, 647 and 649. The isotope pattern around *m*/*z* 647 corresponds to [Zn₂(bomp)(MeCO₂)₂]⁺ (C₂₅H₄₃N₂O₉Zn₂).

Aminopeptidase function

The aminopeptidase activity of complex **1** was estimated using *N*-*p*-nitrophenyl-L-leucine as substrate. Hydrolysis of the amino acid into L-leucine and *p*-nitroaniline was monitored by detecting the latter formed. When a colourless dmf solution of **1** was added to a colourless dmf solution of *N*-*p*-nitrophenyl-L-leucine the solution turned yellow as the result of *p*-nitroaniline formation. This change was observed only in the presence of both **1** and the substrate. Neither the methanolic solution nor an aqueous solution containing zinc(II) ion had aminopeptidase activity. The preliminary aminopeptidase activity of **1** was confirmed in dmf, but a kinetic study was made in water–dmf (6:4) to slow the reaction for experimental convenience. An example of the time course of *p*-nitroaniline formation is shown in Fig. 2. This measurement was made at various complex and substrate concentrations. The results did not obey the Michaelis–Menten theory. This was presumably because **1** was decomposed in parallel in the presence of water and a steady state approximation could not be made. Decomposition of **1** in aqueous media was confirmed by ¹H NMR.
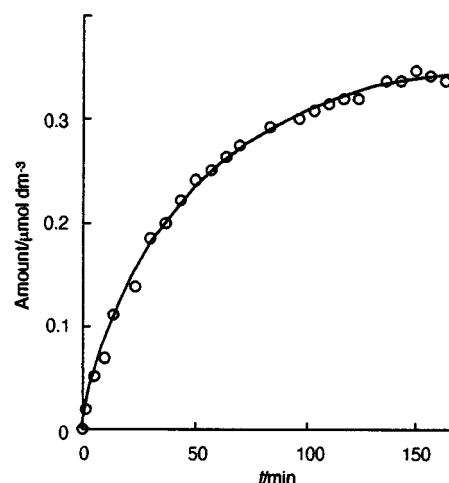

Fig. 2 Time course of *p*-nitroaniline formation in *N*-*p*-nitrophenyl-L-leucine hydrolysis by complex **1**. Conditions: **1** in dmf (3.75×10^{-4} mol dm⁻³, 1 cm³), *N*-*p*-nitrophenyl-L-leucine in Tricine buffer solution (5.0×10^{-4} mol dm⁻³, 1.5 cm³, pH 8), at 25 °C.
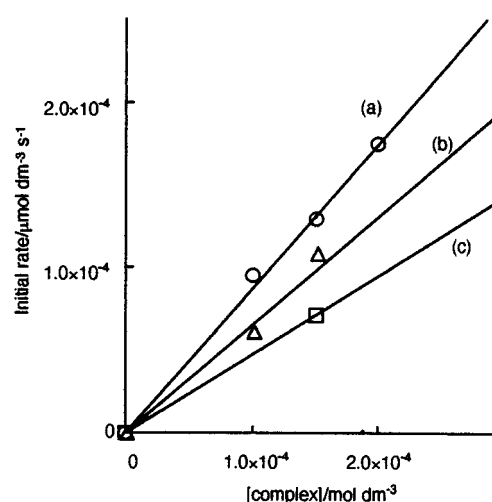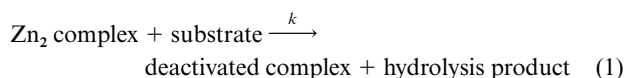

Fig. 3 Correlations between the initial rate and the complex concentration in the hydrolysis of *N*-*p*-nitrophenyl-L-leucine by **1** at 25 °C. *N*-*p*-Nitrophenyl-L-leucine concentration: (a) 4.0×10^{-4}, (b) 3.5×10^{-4} and (c) 2.0×10^{-4} mol dm⁻³.

Thus, the initial rate was obtained graphically from the time course of each experiment. When it is plotted against the complex concentration a good linear correlation is found as shown in Fig. 3. Thus, the initial rate is first order in the complex concentration (initial rate = *k*′[complex]). Similarly, the initial rate of *p*-nitroaniline formation is linearly correlated to the substrate concentration as shown in Fig. 4, *i.e.* the initial rate is first order in the substrate concentration (initial rate = *k*″[substrate]). When (initial rate)/[substrate] is plotted against the complex concentration a good linear correlation holds as shown in Fig. 5. Thus, the initial rate of *p*-nitroaniline formation is first order in both the complex concentration and that of the substrate, *i.e.* initial rate = *k*[complex][substrate] with $k = 2.3(1) \times 10^{-3}$ dm³ mol⁻¹ s⁻¹. This hydrolytic activity of the complex is rather low, but useful as a first step of functional modelling of dinuclear zinc aminopeptidases. Complex **1** decomposed the substrate 0.65 times at most. These results suggest that the active dinuclear zinc species changed to a deactivated species after the substrate hydrolysis as shown in eqn. (1). At this stage the decomposition of **1** was assumed to

$$\text{Zn}_2 \text{ complex + substrate} \xrightarrow{k}$$

$$\text{deactivated complex + hydrolysis product} \quad (1)$$

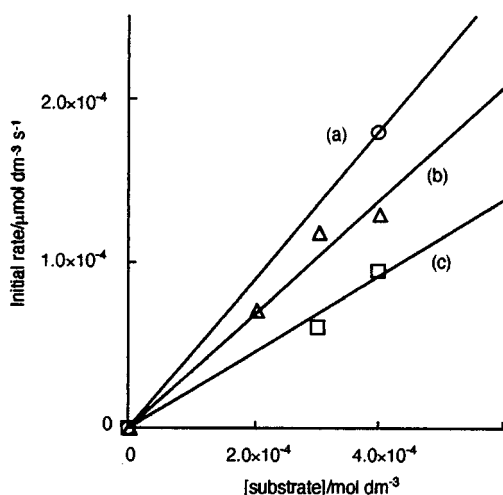be pseudo-first order (rate of decomposition = k'_{decomp}[com-

Fig. 4 Correlations between the initial rate and the substrate concentration in the hydrolysis of *N-p*-nitrophenyl-L-leucine by complex **1** at 25 °C. Concentration of **1**: (a) 2.0×10^{-4}, (b) 1.5×10^{-4} and (c) 1.0×10^{-4} mol dm^{-3}.
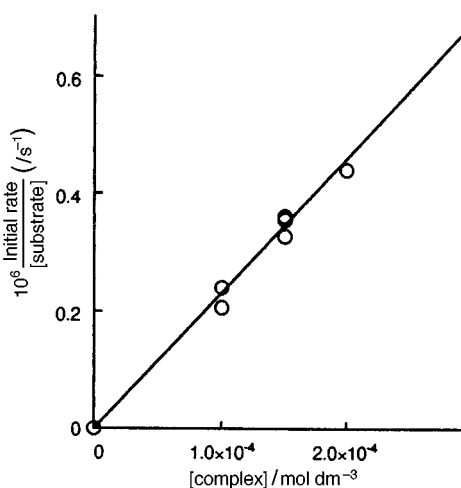

Fig. 5 Correlation between the (initial rate)/[substrate] and the complex concentration in the hydrolysis of *N-p*-nitrophenyl-L-leucine by **1** at 25 °C.

plex]) and the time-course kinetics was examined based on these two parallel reactions [see eqns. (1) and (2)]. All the time

$$\text{Zn}_2 \text{ complex} \xrightarrow{k'_{\text{decomp}}} \text{decomposed species} \qquad (2)$$

courses of *p*-nitroaniline formation were interpreted with $k = 2.5(4) \times 10^{-3}$ dm^3 mol^{-1} s^{-1} and $k'_{\text{decomp}} = 3.3(8) \times 10^{-4}$ s^{-1}. Thus, parallel to the hydrolytic reaction, the decomposition of the dinuclear zinc complex occurs.

However, it is not straightforward to determine the mechanism of this model system from this kinetic measurement. This is because no intermediate species have been detected in this study. The initial complex cation [Zn$_2$(bomp)(MeCO$_2$)$_2$]$^+$ is not an active species since the two zinc(II) ions in it have saturated six-co-ordinate environments which are not suitable for substrate incorporation. In order to clarify the hydrolytic mechanism the development of a new waterproof model system possessing vacant sites for substrate incorporation is necessary.

Conclusion

In this study a new dinuclear zinc(II) complex was reported as the first dizinc functional model of aminopeptidase. Although the aminopeptidase activity of the complex was far from satisfactory, it was useful as a first step of functional modelling of dinuclear zinc aminopeptidases. As a second step it is necessary to design a dinucleating ligand which is also good for substrate incorporation for better aminopeptidase activity.

Acknowledgements

References

1 C. G. Dealwis, L. Chen, C. Brennan, W. Mandecki and C. Abad-Zapatero, *Protein Eng.*, 1995, **8**, 865.
2 Y. Zhang, J. Y. Liang, S. Huang, H. Ke and W. N. Lipscomb, *Biochemistry*, 1993, **32**, 1844.
3 S. K. Burley, P. R. David, A. Taylor and W. N. Lipscomb, *Proc. Natl. Acad. Sci. USA*, 1990, **87**, 6878.
4 S. L. Roderick and B. W. Matthews, *Biochemistry*, 1993, **32**, 3907.
5 B. Chevrier, C. Schalk, H. D'orchymont, J. M. Rondeau, D. Moras and C. Tarnus, *Structure*, 1994, **2**, 283.
6 A. Ishikubo, M. Yashiro and M. Komiyama, *Nucleic Acids Symp. Ser.*, 1995, **34**, 85.
7 C. Bazzicalupi, A. Bencini, A. Bianchi, V. Fusi, C. Giorgi, P. Paoletti, B. Valtancoli and D. Zanchi, *Inorg. Chem.*, 1997, **36**, 2784.
8 M. Suzuki, H. Kanatomi and I. Murase, *Chem. Lett.*, 1981, 1745.
9 M. Suzuki, M. Mikuriya, S. Murata, A. Uehara, H. Oshio, S. Kida and K. Saito, *Bull. Chem. Soc. Jpn.*, 1987, **60**, 4305; A. S. Borovik and L. Que, Jr., *J. Am. Chem. Soc.*, 1988, **110**, 2345; H. Diril, H.-R. Chang, M. J. Nilges, X. Zhang, J. A. Potenza, H. J. Schugar, S. S. Isied and D. H. Hendrickson, *J. Am. Chem. Soc.*, 1989, **111**, 5102; A. S. Borovik, V. Papaefthymiou, L. F. Taylor, O. P. Anderson and L. Que, Jr., *J. Am. Chem. Soc.*, 1989, **111**, 6183; T. R. Holman, C. Juarez-Garcia, M. P. Hendrich, L. Que, Jr., and E. Münck, *J. Am. Chem. Soc.*, 1990, **112**, 7611; M. Ghiladi, C. J. McKenzie, A. Meier, A. K. Powell, J. Ulstrup and K. Wocadlo, *J. Chem. Soc., Dalton Trans.*, 1997, 4011.
10 B. P. Murch, P. D. Boyle and L. Que, Jr., *J. Am. Chem. Soc.*, 1985, **107**, 6728, B. P. Murch, F. C. Bradley, P. D. Boyle, V. Papaefthymiou and L. Que, Jr., *J. Am. Chem. Soc.*, 1987, **109**, 7993.
11 N. Sträter and W. N. Lipscomb, *Biochemistry*, 1995, **34**, 14792.
12 G. Chen, T. Edwards, V. M. D'souza and R. C. Holz, *Biochemistry*, 1997, **36**, 4278.
13 A. Altomare, M. C. Burla, M. Camalli, M. Cascarano, C. Giacovazzo, A. Guagliardi and G. Polidori, *J. Appl. Crystallogr.*, 1994, **27**, 435.
14 P. T. Beurskens, G. Admiraal, G. Beurskens, W. P. Bosman, R. de Geder, R. Israel and J. M. M. Smits, The DIRDIF 94 program system, Technical Report of the Crystallography Laboratory, University of Nijmegen, 1994.
15 D. T. Cromer and J. T. Waber, *International Tables for X-Ray Crystallography*, Kynoch Press, Birmingham, 1974, vol. IV, Table 2.2 A.
16 TEXSAN, Crystal Structure Analysis Package, Molecular Structure Corporation, Houston, TX, 1985 and 1992.
17 C. K. Johnson, ORTEP, Report ORNL 5138, Oak Ridge National Laboratory, Oak Ridge, TN, 1976.
18 G. B. Deacon and R. J. Phillips, *Coord. Chem. Rev.*, 1980, **32**, 227.

Paper 8/08055K